



## Search for the $K^-pp$ bound state via $\gamma d \rightarrow K^+\pi^-X$ reaction at $E_\gamma = 1.5\text{--}2.4$ GeV



LEPS Collaboration

A.O. Tokiyasu<sup>a,\*</sup>, M. Niiyama<sup>b</sup>, J.D. Parker<sup>b</sup>, D.S. Ahn<sup>a</sup>, J.K. Ahn<sup>c</sup>, S. Ajimura<sup>a</sup>, H. Akimune<sup>d</sup>, Y. Asano<sup>e</sup>, W.C. Chang<sup>f</sup>, J.Y. Chen<sup>a</sup>, S. Daté<sup>g</sup>, H. Ejiri<sup>a</sup>, H. Fujimura<sup>ae</sup>, M. Fujiwara<sup>a,i</sup>, S. Fukui<sup>j</sup>, S. Hasegawa<sup>a</sup>, K. Hicks<sup>k</sup>, K. Horie<sup>a</sup>, T. Hotta<sup>a</sup>, S.H. Hwang<sup>l</sup>, K. Imai<sup>l</sup>, T. Ishikawa<sup>h</sup>, T. Iwata<sup>m</sup>, Y. Kato<sup>n</sup>, H. Kawai<sup>o</sup>, K. Kino<sup>a</sup>, H. Kohri<sup>a</sup>, Y. Kon<sup>a</sup>, N. Kumagai<sup>g</sup>, D.L. Lin<sup>f</sup>, Y. Maeda<sup>a</sup>, S. Makino<sup>p</sup>, T. Matsuda<sup>q</sup>, T. Matsumura<sup>r</sup>, N. Matsuoka<sup>a</sup>, T. Mibe<sup>a</sup>, M. Miyabe<sup>h</sup>, M. Miyachi<sup>s</sup>, N. Muramatsu<sup>h</sup>, R. Murayama<sup>t</sup>, T. Nakano<sup>a</sup>, Y. Nakatsugawa<sup>a</sup>, M. Nomachi<sup>t</sup>, Y. Ohashi<sup>g</sup>, H. Ohkuma<sup>g</sup>, T. Ohta<sup>a</sup>, T. Ooba<sup>o</sup>, D.S. Oshuev<sup>f</sup>, C. Rangacharyulu<sup>u</sup>, S.Y. Ryu<sup>a,c</sup>, A. Sakaguchi<sup>t</sup>, T. Sawada<sup>a</sup>, P.M. Shagin<sup>v</sup>, Y. Shiino<sup>o</sup>, H. Shimizu<sup>h</sup>, E.A. Strokovsky<sup>ac</sup>, Y. Sugaya<sup>t</sup>, M. Sumihama<sup>w</sup>, J.L. Tang<sup>ad</sup>, Y. Toi<sup>q</sup>, H. Toyokawa<sup>g</sup>, T. Tsunemi<sup>b</sup>, M. Uchida<sup>x</sup>, M. Ungaro<sup>ab</sup>, A. Wakai<sup>y</sup>, C.W. Wang<sup>f</sup>, S.C. Wang<sup>f</sup>, K. Yonehara<sup>d</sup>, T. Yorita<sup>a,g</sup>, M. Yoshimura<sup>z</sup>, M. Yosoi<sup>a</sup>, R.G.T. Zegers<sup>aa</sup>

<sup>a</sup> Research Center for Nuclear Physics, Osaka University, Ibaraki, Osaka 567-0047, Japan<sup>b</sup> Department of Physics, Kyoto University, Kyoto 606-8502, Japan<sup>c</sup> Department of Physics, Pusan National University, Busan 609-735, Republic of Korea<sup>d</sup> Department of Physics, Konan University, Kobe, Hyogo 658-8501, Japan<sup>e</sup> XFEL Project Head Office, RIKEN 1-1, Koto, Sayo, Hyogo 679-5148, Japan<sup>f</sup> Institute of Physics, Academia Sinica, Taipei 11529, Taiwan<sup>g</sup> Japan Synchrotron Radiation Research Institute, Sayo, Hyogo 679-5143, Japan<sup>h</sup> Research Center for Electron Photon Science, Tohoku University, Sendai, Miyagi 982-0826, Japan<sup>i</sup> Advanced Photon Research Center, Japan Atomic Energy Agency, Kizugawa, Kyoto 619-0215, Japan<sup>j</sup> Department of Physics and Astrophysics, Nagoya University, Nagoya, Aichi 464-8602, Japan<sup>k</sup> Department of Physics And Astronomy, Ohio University, Athens, OH 45701, USA<sup>l</sup> Advanced Science Research Center (ASRC), Japan Atomic Energy Agency (JAEA), Tokai, Ibaraki 319-1195, Japan<sup>m</sup> Department of Physics, Yamagata University, Yamagata 990-8560, Japan<sup>n</sup> Division of Particle and Astrophysical Sciences, Nagoya University, Furo-cho, Chikusa-ku, Nagoya-shi 464-6802, Japan<sup>o</sup> Department of Physics, Chiba University, Chiba 263-8522, Japan<sup>p</sup> Wakayama Medical College, Wakayama, Wakayama 641-8509, Japan<sup>q</sup> Department of Applied Physics, Miyazaki University, Miyazaki 889-2192, Japan<sup>r</sup> Department of Applied Physics, National Defense Academy in Japan, Yokosuka, Kanagawa 239-8686, Japan<sup>s</sup> Department of Physics, Tokyo Institute of Technology, Tokyo 152-8551, Japan<sup>t</sup> Department of Physics, Osaka University, Toyonaka, Osaka 560-0043, Japan<sup>u</sup> Department of Physics and Engineering Physics, University of Saskatchewan, Saskatoon, SK S7N 5E2, Canada<sup>v</sup> School of Physics and Astronomy, University of Minnesota, Minneapolis, MN 55455, USA<sup>w</sup> Department of Education, Gifu University, Gifu 501-1193, Japan<sup>x</sup> Department of Physics, Tokyo Institute of Technology, Tokyo 152-8551, Japan<sup>y</sup> Akita Research Institute of Brain and Blood Vessels, Akita 010-0874, Japan<sup>z</sup> Institute for Protein Research, Osaka University, Suita, Osaka 565-0871, Japan<sup>aa</sup> National Superconducting Cyclotron Laboratory, Michigan State University, East Lansing, MI 48824, USA<sup>ab</sup> Department of Physics, University of Connecticut, Storrs, CT 06269-3046, USA<sup>ac</sup> Joint Institute for Nuclear Research, RU-141980 Dubna, Russia<sup>ad</sup> Department of Physics, National Chung Cheng University, Taiwan<sup>ae</sup> School of Medicine, Wakayama Medical University, Wakayama 641-0011, Japan

\* Corresponding author.

## ARTICLE INFO

## Article history:

Received 25 June 2013

Received in revised form 21 November 2013

Accepted 12 December 2013

Available online 17 December 2013

Editor: V. Metag

## Keywords:

Kaonic nuclei

Antikaon-nucleon physics

Photo-production

## ABSTRACT

A search for the  $K^-pp$  bound state (the lightest kaonic nucleus) has been performed using the  $\gamma d \rightarrow K^+\pi^-X$  reaction at  $E_\gamma = 1.5\text{--}2.4$  GeV at LEPS/SPring-8. The differential cross section of the  $K^+\pi^-$  photo-production off deuterium ( $d^2\sigma/d\cos\theta_{K^+}^{lab}/d\cos\theta_{\pi^-}^{lab}$ ) has been measured for the first time in this energy region. A peak structure was searched for in the inclusive missing mass spectrum. A statistically significant peak structure was not observed in the region from 2.22 to 2.36 GeV/ $c^2$ . The upper limits of the differential cross section of the  $K^-pp$  bound state production were determined to be (0.17–0.55), (0.55–1.7) and (1.1–2.9)  $\mu b$  at 95% confidence level with the assumed widths of 20 MeV, 60 MeV and 100 MeV.

© 2013 The Authors. Published by Elsevier B.V. Open access under CC BY license.

## 1. Introduction

Kaonic nuclei provide us with rich information on the sub-threshold  $\bar{K}N$  interaction and the nature of  $\Lambda(1405)$  in the nuclear medium. Since the  $\bar{K}N$  interaction is strongly attractive in the isospin 0 channel, the existence of kaonic nuclei is supported theoretically. Many experiments have been performed to search for kaonic nuclei using various reactions. KEK-PS E471/E549 group searched for the four-body systems: the  $K^-ppn$  and  $K^-pn\bar{n}$  bound state using the stopped  $K^-$  reaction on a liquid  ${}^4He$  target [1,2]. Narrow (the width is less than 40 MeV) peaks were not observed in the missing mass spectra of  ${}^4He(K_{stopped}^-, p)X$  and  ${}^4He(K_{stopped}^-, n)X$ , and they concluded that the upper limits of the formation probability are below a few percent per stopped  $K^-$  events. However, they observed broad structures at around 3140 MeV/ $c^2$  in the missing mass spectrum of  ${}^4He(K_{stopped}^-, n)X$ . It cannot be completely explained in terms of two-nucleon absorption processes, implying the possible existence of unknown processes including the  $K^-ppn$  bound state. Osaka group studied the  $\bar{K}$ -nucleus interaction using in-flight ( $K^-, N$ ) reactions on  ${}^{12}C$  and  ${}^{16}O$  targets [3,4]. An enhancement of the yield in the  $K^-$  bound region was observed in the inclusive missing mass spectra. The shapes of the obtained spectra were compared with theoretical calculations, and the  $\bar{K}$  potential were derived to be rather deep (160–190 MeV). However, another theoretical calculation explained the spectra with a shallow (60 MeV) potential [5], and more intensive experimental investigations are needed to improve the precision of the shape analysis.

The lightest kaonic nuclei,  $\bar{K}NN$  is fascinating to investigate the sub-threshold  $\bar{K}N$  interaction more precisely. In particular, the bound state consisting of  $K^-$  and two protons (the  $K^-pp$  bound state) has been actively studied because it has the largest number of  $\bar{K}N$  pairs with  $I = 0$  and is estimated to be the strongest binding system among the three-body systems.

The structure and the production mechanism of the  $K^-pp$  bound state have been investigated using various theoretical approaches [6–12]. The binding energy (B.E.) and the width ( $\Gamma$ ) were predicted to be 9–95 MeV and 34–110 MeV, respectively. The predicted values are in considerable disagreement among the theoretical models depending on the  $\bar{K}N$  interaction models and the calculation methods. The  $K^-pp$  bound state has been searched for experimentally, and there are two groups who have detected the possible candidates. The first measurement was reported by FINUDA group at DAΦNE [13]. They investigated the stopped  $K^-$  reaction on five kinds of targets of  ${}^6Li$ ,  ${}^7Li$ ,  ${}^{12}C$ ,  ${}^{27}Al$  and  ${}^{51}V$  and observed a peak structure in the invariant mass spectrum of  $\Lambda$  and proton emitted back-to-back from the targets. The B.E. and  $\Gamma$  were determined to be  $115^{+6}_{-5}(stat)^{+3}_{-4}(syst)$  MeV and  $67^{+14}_{-11}(stat)^{+2}_{-3}(syst)$  MeV, respectively. There are some theoretical interpretations that the observed peak can be explained by the two-nucleon absorption

with the final state interaction of outgoing particles [14]. DISTO group at SATURNE re-analyzed the dataset of the exclusive  $pp \rightarrow pK^+\Lambda$  reaction and observed a peak structure in the missing mass spectrum of  $K^+$  [15]. The B.E. and  $\Gamma$  were determined as  $103 \pm 3(stat) \pm 5(syst)$  MeV and  $118 \pm 8(stat) \pm 10(syst)$  MeV, respectively. These two measured values of B.E. and  $\Gamma$  are different from each other. They are inconsistent with any of the existing theoretical predictions. Thus, the existence of the  $K^-pp$  bound state has not been established yet. New experiments using different reactions could help to resolve the controversial situation.

In this Letter, we report on the first search results using the  $\gamma d \rightarrow K^+\pi^-X$  reaction in the photon energy region of  $E_\gamma = 1.5\text{--}2.4$  GeV. A peak structure was searched for in the inclusive missing mass spectrum of the  $d(\gamma, K^+\pi^-)X$  reaction ( $MM_d(K^+\pi^-)$ ) by detecting  $K^+$  and  $\pi^-$  at forward angles in coincidence. The study of the inclusive spectrum allowed us to search for the  $K^-pp$  bound state without selecting the decay mode, whereas considerable contributions from quasi-free processes arise as the background in the search region ranging from 2.22 GeV/ $c^2$  to 2.36 GeV/ $c^2$ . These background processes are also discussed.

If  $K^+$  is detected at forward angles,  $t$ -channel reaction becomes dominant.  $\bar{K}$  or  $K^*$  are expected to be exchanged in the framework of gauge-invariant effective Lagrangians [16]. A  $\bar{K}$  exchange is forbidden in the pion or kaon induced reactions, and it is one of the unique features of the photon induced reaction. Here, the exchanged  $\bar{K}$  or  $K^*$  can be treated as virtual beam particles. From this viewpoint,  $d(\gamma, K^+\pi^-)X$  reaction is regarded as the virtual  $d(K^-, \pi^-)X$  or  $d(K^*, \pi^-)X$  reaction, which have not yet been used for the search for the  $K^-pp$  bound state.

The production cross section of the  $K^-pp$  bound state is described as a function of the transferred momentum,  $|t|$  [17]. If the  $K^-pp$  bound state is a compact object, the production cross section is expected to be enlarged at a large transferred momentum. On the other hand, if the  $K^-pp$  bound state is a soft object, the production cross section is expected to be enlarged at a small transferred momentum. By detecting  $K^+$  and  $\pi^-$  at forward angles, we searched for the  $K^-pp$  bound state in the small  $|t|$  region from 0.1 to 0.4 (GeV/ $c^2$ ).

## 2. The LEPS experiment and analysis

The experiment was performed at LEPS/SPring-8 in 2002/2003 and 2006/2007. The experimental conditions and data qualities were similar throughout these two data-taking periods. Therefore two datasets were summed up for the analysis. Linearly polarized photons with the energy from 1.5 to 2.4 GeV were produced by the backward Compton scattering. The energy of each photon was measured by detecting the scattered electrons with a tagging counter. The photon energy resolution is estimated to be approximately 12 MeV. More details of the photon beam at LEPS/SPring-8 are given in Ref. [18].

Liquid deuterium ( $\text{LD}_2$ ) of 16 cm effective length was used as the target.  $7.6 \times 10^{12}$  tagged photons were incident on the target in total. Charged particles produced from the target were detected with the LEPS spectrometer at forward angles in the laboratory system. The LEPS spectrometer consists of a start counter (SC), a silica-aerogel Čerenkov counter (AC), a silicon vertex detector (SVTX), drift chambers (DCs), a dipole magnet with a field strength of 0.7 T and a time-of-flight (TOF) scintillator wall. AC has the refractive index 1.03 and was used for  $e^+e^-$  vetoes at the trigger level. The momentum threshold of AC is 2.0  $\text{GeV}/c$  for kaons and 0.57  $\text{GeV}/c$  for pions. The momenta of particles were determined using tracking information, and particle species were identified using TOF information. The momentum resolution is estimated to be 6  $\text{MeV}/c$  at 1  $\text{GeV}/c$  by the Monte Carlo simulation. Thus, the mass resolution of  $MM_d(K^+\pi^-)$  is  $\sim 10 \text{ MeV}/c^2$  in the region from 2.2 to 2.4  $\text{GeV}/c^2$ . More details about the experimental setup are given in [19].

For the present analysis, events with  $K^+$  and  $\pi^-$  tracks were selected with mass values required to be within  $3\sigma$ , where  $\sigma$  is the mass resolution depending on the momentum. Events for which  $\pi^+$  was misidentified as  $K^+$  were rejected by requiring that the missing mass of the  $p(\gamma, \pi^+\pi^-)X$  reaction was above 0.97  $\text{GeV}/c^2$ , where the  $\pi^+$  mass was used instead of the  $K^+$  mass. The misidentified events were distributed mainly in the region below 1.7  $\text{GeV}/c^2$  in the  $MM_d(K^+\pi^-)$  spectrum and were negligible in the region where a peak structures was searched for. To reduce the systematic uncertainty arising from the acceptance correction, the analysis was performed within the following kinematical region:

$$\begin{aligned} \cos\theta_{K^+}^{\text{lab}} &> 0.95 \\ \cos\theta_{\pi^-}^{\text{lab}} &> 0.95 \\ 0.25 \text{ GeV}/c < p_{K^+}^{\text{lab}} &< 2.0 \text{ GeV}/c \\ 0.25 \text{ GeV}/c < p_{\pi^-}^{\text{lab}} &< 0.6 \text{ GeV}/c \end{aligned} \quad (1)$$

Here  $\theta^{\text{lab}}$  and  $p^{\text{lab}}$  denotes the scattering angle and momentum in the laboratory system, respectively. The vertex resolution along the beam axis was approximately 2 mm, and the events from the SC or AC were well-separated from the events from the  $\text{LD}_2$  target. The vertex points of the  $K^+$  and  $\pi^-$  tracks were required to be located at the target. In addition, the distance of closest approach (DCA) between the two tracks was required to be less than 4 mm. These vertex constraints reduced the contribution of the hyperon decay events of which vertex points were outside the target or had large DCA values. The ratio of the signal of the  $K^-pp$  bound state to the background arising from the hyperon decay events was estimated to be improved by a factor of 2 by applying these vertex constraints. The event loss of the signal of the  $K^-pp$  bound state by these constraint was estimated to be 5% by the Monte Carlo simulation. Finally, for the events in which three tracks were detected ( $K^+$ ,  $\pi^-$ , and  $p$ ), the invariant masses of  $p$  and  $\pi^-$  ( $M(p\pi^-)$ ) were calculated, and the events in the range of  $1.05 \text{ GeV}/c^2 < M(p\pi^-) < 1.12 \text{ GeV}/c^2$  were rejected because they arise from the quasi-free  $\Lambda$  production process. The event loss due to this cut is small ( $\sim 4\%$ ). There is little possibility to distort the shape of the spectrum of  $MM_d(K^+\pi^-)$ .

### 3. Results and discussion

Fig. 1 shows the differential cross section spectrum of  $MM_d(K^+\pi^-)$  ( $d^3\sigma/d\cos\theta_{K^+}^{\text{lab}}/d\cos\theta_{\pi^-}^{\text{lab}}/dM$ ) within the kinematical region given in Eq. (1). The search region ( $2.22 \text{ GeV}/c^2$ – $2.36 \text{ GeV}/c^2$ ) and the  $K^-pp$  mass threshold ( $2.37 \text{ GeV}/c^2$ ) are also indicated in the figure.

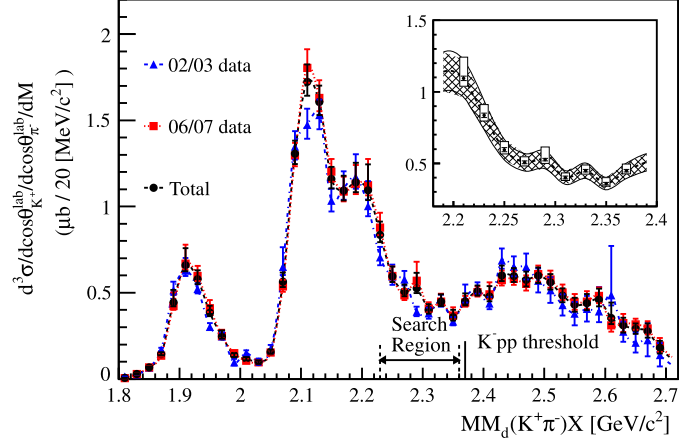


**Fig. 1.** (Color online.) Differential cross section of  $d(\gamma, K^+\pi^-)X$ ,  $d^3\sigma/d\cos\theta_{K^+}^{\text{lab}}/d\cos\theta_{\pi^-}^{\text{lab}}/dM$ . The bin width is 20  $\text{MeV}/c^2$ . The blue triangle points denote the results of 2002/2003 dataset, the red square 2006/2007 dataset and the back circle summed up dataset. The error bars include both statistical and systematic errors. Inset: The differential cross section in the range from 2.2 to 2.4  $\text{GeV}/c^2$ . The error bars and the open boxes indicate statistical and systematic errors, respectively. The error band denotes the discrepancy between two datasets.

The differential cross section was obtained by applying an acceptance correction for each event. The acceptance was calculated with the GEANT-based Monte Carlo simulation as a function of momentum,  $\cos\theta^{\text{lab}}$  and vertex point. The systematic uncertainty arising from the acceptance correction is estimated to be 5.7% in the search region. The fluctuation of the target density was assumed to be negligibly small. The systematic uncertainty of photon flux was estimated to be 3%. The systematic uncertainty arising from the above-mentioned sources was 6.4% in total in the search region. There was discrepancy in the obtained results between the two datasets. The discrepancy is estimated to be 12% (R.M.S.) using the quasi-free  $\Lambda$  and  $\Sigma$  production, which is shown as a error band in the inset in Fig. 1. The results obtained from two datasets were consistent within this error.

As shown in Fig. 1, there are three peaks around 1.9  $\text{GeV}/c^2$ , 2.1  $\text{GeV}/c^2$  and 2.2  $\text{GeV}/c^2$  in the  $MM_d(K^+\pi^-)$  spectrum. These peaks correspond to the  $\gamma n \rightarrow K^+\Sigma^-$  followed by the  $\Sigma^- \rightarrow \pi^-n$ , the  $\gamma n \rightarrow K^+\pi^-\Lambda$  and the  $\gamma p/n \rightarrow K^+\pi^-\Sigma^{+/0}$  processes. The differential cross section of each process was determined to be  $\sim 3 \mu\text{b}$ ,  $\sim 7 \mu\text{b}$  and  $\sim 4 \mu\text{b}$ , respectively, within the kinematical region given in Eq. (1). If the  $K^-pp$  bound state exists and has a large production rate, a peak structure should be observed as the signal in the range from 2.22  $\text{GeV}/c^2$  to 2.36  $\text{GeV}/c^2$  in the  $MM_p(K^+\pi^-)$  spectrum.

A peak structure corresponding to the  $K^-pp$  bound state production was searched for with the Log-likelihood ratio method. In this method, firstly, the  $MM_d(K^+\pi^-)$  spectrum was fitted under two hypotheses: background processes only, and background processes and the signal process of the  $K^-pp$  bound state production. Then, the improvement of the Log-likelihood value was tested. For the fitting, we use the spectrum without the acceptance correction (raw spectrum) and the Monte Carlo generated spectra of the assumed processes as the fitting function. The reasons why we use the raw spectrum are as follows. As shown in the inset of Fig. 1, the spectrum has considerable systematic uncertainties coming from the acceptance correction. The acceptance correction was performed for each track to derive the differential cross section, and the uncertainty attributed for each event was accumulated to the final result. On the other hand, in case of the Monte Carlo generated spectra, we can easily reduce the systematic uncertainties by increasing the statistics of the generated

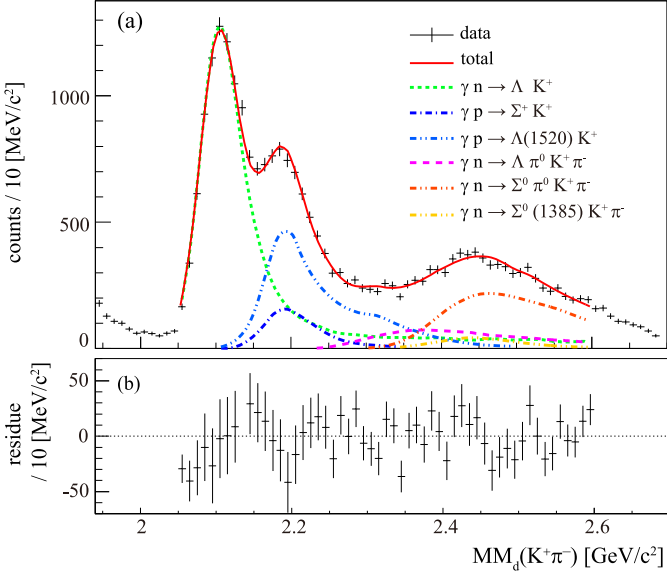


**Fig. 2.** (Color online.) (a) The fit result of  $MM_d(K^+\pi^-)$  spectrum with the Monte Carlo generated processes. The color and style of line for each corresponding process are shown. (b) The residue from the fitting function.

events. The Monte Carlo generated spectra were estimated to have the systematic uncertainty  $\sim 1\%$ . By using the raw spectrum and the Monte Carlo generated spectra for the fitting, we can avoid the ambiguity arising from the acceptance correction for each track. In addition, by using Monte Carlo generated spectra, we can take into account of the mass resolution effectively.

The fitting was performed in the range from 2.05 to 2.6 GeV/c<sup>2</sup>. Six processes were used for the background:  $\gamma n \rightarrow \Lambda K^+ \pi^-$ ,  $\gamma p \rightarrow \Sigma^+ K^+ \pi^-$ ,  $\gamma p \rightarrow \Lambda(1520) K^+$ ,  $\gamma n \rightarrow \Lambda \pi^0 K^+ \pi^-$ ,  $\gamma n \rightarrow \Sigma^0 \pi^0 K^+ \pi^-$  and  $\gamma p \rightarrow \Sigma^0(1385) K^+ \pi^-$ . The shapes of the spectra were generated with the GEANT-based Monte Carlo simulation, where the Paris-potential model was used to describe the momentum distribution of the nucleons inside the deuteron [20]. The yield of each background process was taken into account as a free parameter. The yield of the signal was increased from 0 to a certain value, and the Log-likelihood values was calculated at each point.

Fig. 2 shows the fit result with only background processes and the residue from the fitting function.  $\chi^2/ndf$  of the fit result is 1.4 in the range from 2.05 GeV/c<sup>2</sup> to 2.6 GeV/c<sup>2</sup>, and approximately 1 in the range from 2.22 GeV/c<sup>2</sup> to 2.36 GeV/c<sup>2</sup>. The tests were performed for signals with  $\Gamma = 20, 60$  and  $100$  MeV, and 15 B.E. values ranging from 10 to 150 MeV. The signal shape was assumed to be the Breit-Wigner distribution with the fixed B.E. and  $\Gamma$  and was generated with the GEANT-based Monte Carlo simulation. As a result of tests, significant decrease of  $-2\Delta \ln L$  (twice the Log-likelihood difference of the hypotheses) were not observed under any assumption of B.E. and  $\Gamma$  values.

To quantify the search results, the upper limits of the differential cross section of the  $K^-pp$  bound state production were determined. The signal yield which gave  $-2\Delta \ln L = 3.84$  was used for the upper limit of the yield at the 95% confidence level. In Fig. 3,  $-2\Delta \ln L$  values are shown as a function of the signal yield for B.E. = 100 MeV and  $\Gamma = 60$  MeV as a typical example.

The obtained yields were converted to the differential cross section by dividing them by the acceptance of the signals, efficiencies and integrated luminosities. The acceptance of the signal was determined by using the GEANT-based Monte Carlo simulation under the assumption that the  $d(\gamma, K^+\pi^-)K^-pp$  reaction occurs isotropically in the center-of-mass system. The systematic error from this

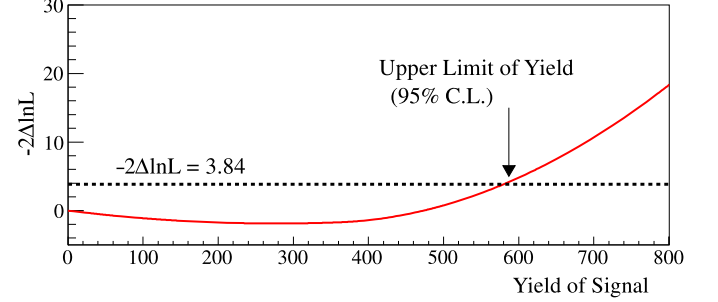


**Fig. 3.** (Color online.) Typical  $-2\Delta \ln L$  values as a function of the signal yield. The B.E. and  $\Gamma$  values were assumed to be 100 MeV and 60 MeV, respectively. The crossing point at  $-2\Delta \ln L = 3.84$  is indicated by an arrow.

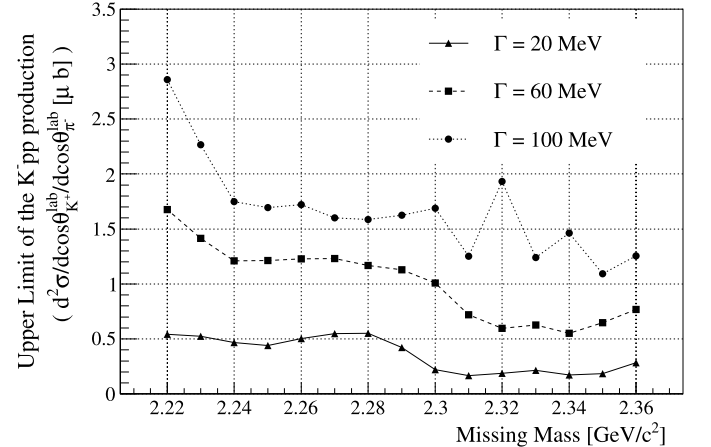


**Fig. 4.** The upper limit of the differential cross section of the  $K^-pp$  bound state production in the  $d(\gamma, K^+\pi^-)X$  reaction as a function of assumed signal peak mass. The solid, broken and dotted lines are the results of  $\Gamma = 20$  MeV, 60 MeV and 100 MeV, respectively.

acceptance was estimated to be  $\sim 1\%$ . Fig. 4 shows the upper limits of the differential cross section of the  $K^-pp$  bound state production for various  $\Gamma$  values as a function of the assumed mass. It is noted that the obtained upper limit of the differential cross section has  $\sim 12\%$  uncertainty mainly coming from the discrepancy between two datasets. In addition, we performed the same analyses by using some different combinations for the background processes. Among them, the combination which gave the most conservative results of the upper limits was adopted.

The upper limits of the differential cross section of the  $K^-pp$  bound state production were determined to be (0.17–0.55), (0.55–1.7) and (1.1–2.9)  $\mu b$  for  $\Gamma = 20, 60$  and  $100$  MeV, respectively at the 95% confidence level. These values correspond to (1.5–5.0), (5.0–15) and (9.9–26)% of the differential cross section of the typical hadron production processes such as the  $\gamma n \rightarrow K^+\pi^- \Lambda$  or the  $\gamma p/n \rightarrow K^+\pi^- \Sigma^{+0}$  processes within the kinematical region given in Eq. (1). As for the upper limits for  $\Gamma = 20$  MeV, we can compare the obtained results with those given by the KEK-PS E471/E549 group. The differences between the present and the KEK-PS E471/E549 experiment are summarized as follows:

- The search object of the present study is the  $K^-pp$  bound state, while the KEK-PS E471/E549 experiment aimed at the  $K^-ppn$  or  $K^-pnn$  bound states.
- The production mechanisms of kaonic nuclei are expected to be different between the photon induced and stopped  $K^-$  reactions.

**Table 1**  
Quasi-free processes.

Proton target	Neutron target
$\gamma + p \rightarrow \Lambda K^+$	$\gamma + n \rightarrow \Sigma^- K^+$
$\gamma + p \rightarrow \Sigma^0 K^+$	$\gamma + n \rightarrow \Lambda K^+ \pi^-$
$\gamma + p \rightarrow \Lambda(1405) K^+$	$\gamma + n \rightarrow \Sigma(1385)^- K^+$
$\gamma + p \rightarrow \Sigma(1385)^0 K^+$	$\gamma + n \rightarrow \Sigma(1660)^- K^+$
$\gamma + p \rightarrow \Sigma^+ K^+ \pi^-$	$\gamma + n \rightarrow \Lambda \pi^0 K^+ \pi^-$
$\gamma + p \rightarrow \Lambda(1520) K^+$	
$\gamma + p \rightarrow \Sigma^0 \pi^+ K^+ \pi^-$	

- The present study is limited within the kinematical region given in Eq. (1).

However, two experiments are similar to each other in the aspect that peak structures were searched for in the inclusive missing mass spectra. KEK-PS E471/E549 group concluded that the formation probabilities of the four-body kaonic nuclei with narrow widths are less than a few percent per stopped kaon. Since absorbed  $K^-$  in nuclei forms hyperons, their results are restated that the formation probabilities of kaonic nuclei are less than a few percent of the typical hyperon production cross section. The present results with an assumption of  $\Gamma = 20$  MeV are comparable with the KEK results in terms of the ratio to the hyperon production cross section.

Though a peak structures was not observed, there were several thousand events in the search region. To investigate the background precisely, the  $MM_p(K^+ \pi^-)$  spectrum and the  $MM_p(K^+)$  spectrum were fitted simultaneously. The subscript “*p*” means that the missing mass was calculated using the proton mass for the target mass. The processes used for the fitting are listed in Table 1. The contribution of  $K^{*0}$  production is negligibly small under the selected kinematic conditions and was ignored. PDG values were used for the mass, the width and the branching ratio of the hyperon resonances [21], and all the processes were generated isotropically in the center of mass system in the Monte Carlo simulation. The mass and width of  $\Sigma(1660)$  were assumed to be 1.66 GeV/c<sup>2</sup> and 0.1 GeV, respectively, and the branching ratios of the  $\Lambda \pi^-$  and  $\Sigma \pi^-$  decay modes were taken into account as free parameters. The fit result is shown in Fig. 5. The experimental data is shown as points with the error bars, and the fit results are shown as the red histograms. The total  $\chi^2/\text{ndf}$  for the fitting was 1.3. The fit result indicates that the main contribution to the  $MM_d(K^+ \pi^-)$  spectrum in the search region comes from the  $\gamma p \rightarrow K^+ \Lambda(1520)$  process. Its fraction of the observed yield is  $22 \pm 3\%$ . The contribution of the non-resonant  $\Lambda/\Sigma \pi^+ K^+ \pi^-$  production is also estimated to be  $24 \pm 5\%$  in the search region.

The production cross section of the  $K^- pp$  bound state was found to be small in the photon induced reaction, and it is difficult to separate the  $K^- pp$  bound state signal from the background processes in the inclusive measurement. For the further study, it is necessary to detect the decay products of the  $K^- pp$  bound state using the additional counters surrounding the target. The  $K^- pp$  bound state is expected to have non-mesonic decay modes such as the  $K^- pp \rightarrow \Lambda p$  or the  $K^- pp \rightarrow \Sigma N$ . In this case, the detection of proton or  $\Lambda$  with a large transverse momentum is essential to reduce the contribution of background processes.

In addition to the search under the cut condition given in Eq. (1), searches for a peak structure were done in the different kinematical conditions as follows: (a)  $|t| < 0.3$  (GeV/c)<sup>2</sup>, (b)  $p_X < 0.8$  GeV/c and (c)  $0.842 \text{ GeV}/c^2 < M(K^+ \pi^-) < 0.942 \text{ GeV}/c^2$ . Here,  $p_X$  is the transferred momentum in the virtual  $d(K^-, \pi^-)X$  reaction, and  $M(K^+ \pi^-)$  is the invariant mass of  $K^+$  and  $\pi^-$ . The cut conditions (a) and (b) correspond to selecting the especially small transferred momentum. The production cross section of the

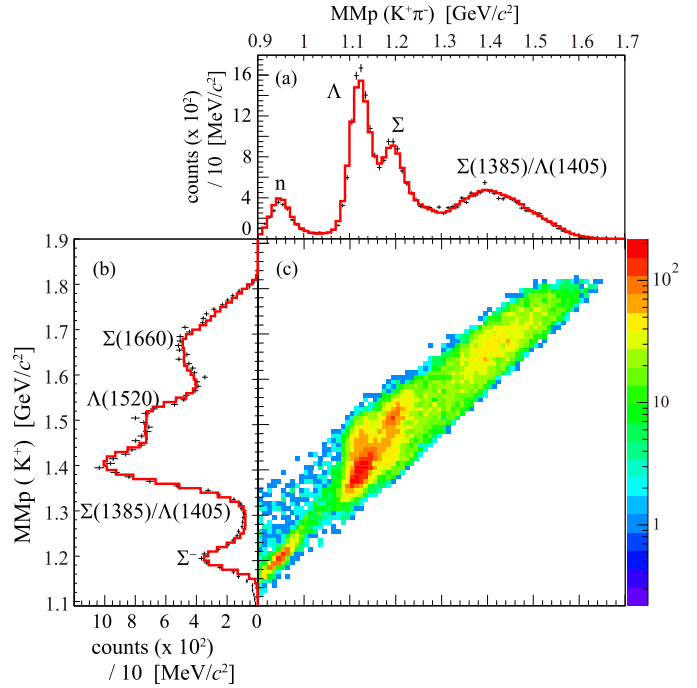


**Fig. 5.** (Color online.) Simultaneous fit result of (a)  $MM_p(K^+ \pi^-)$  and (b)  $MM_p(K^+)$ . The processes used for fitting are listed in Table 1. The points with error bar denotes the observed histogram, and the red histogram denotes the summation of contribution from each process after the fit. (c) The scatter plot of  $MM_p(K^+ \pi^-)$  and  $MM_p(K^+)$ .

$K^- pp$  bound state is dependent on the kinematic condition, especially transferred momentum of the residual system. Although the production mechanism of the  $K^- pp$  bound state is poorly understood, if the  $K^- pp$  bound state was produced via the sticking process of the virtual  $K^-$  or intermediate resonance states, the kinematic condition of small transferred momentum is expected to enlarge the production cross section. The cut condition (c) corresponds to selecting  $K^{*0}$  production events. By applying the cut condition (c), the  $K^- pp$  bound state was searched for in a different reaction channel: the  $d(\gamma, K^{*0})X$  reaction. If  $K^{*0}$  is produced at forward angles, the exchanged particle in the  $t$ -channel is limited to  $\bar{K}$  and  $\kappa$  [22]. A peak structure was searched for in the  $MM_d(K^+ \pi^-)$  spectrum under the conditions (a), (b) and (c), but no structure was observed again.

#### 4. Conclusion

We searched for the  $K^- pp$  bound state using the  $\gamma d \rightarrow K^+ \pi^- X$  reaction at  $E_\gamma = 1.5\text{--}2.4$  GeV.  $K^+$  and  $\pi^-$  were detected at forward angles. The differential cross section of the  $K^+ \pi^-$  photo-production off deuterium was measured for the first time in this energy region. A peak structure corresponding to the  $K^- pp$  bound state was searched for in the inclusive  $MM_d(K^+ \pi^-)$  spectrum with the Log-likelihood ratio method. No peak structure was observed in the region from 2.22 to 2.36 GeV/c<sup>2</sup>, and the upper limits of the differential cross section of the  $K^- pp$  bound state production were determined to be (0.17–0.55), (0.55–1.7) and (1.1–2.9)  $\mu\text{b}$  at 95% confidence level for  $\Gamma = 20, 60$  and  $100$  MeV, respectively. These values correspond to approximately 1.5–20% of the cross section of the typical hyperon photo-production. To study the origin of the background, the  $MM_p(K^+ \pi^-)$  spectrum and the  $MM_p(K^+)$  spectrum were fitted simultaneously by including 15 background processes. The  $\gamma p \rightarrow K^+ \Lambda(1520)$  process

and the  $\gamma N \rightarrow K^+ \pi^- \pi \Lambda/\Sigma$  process were found to be the main contribution in the region from 2.22 to 2.36  $\text{GeV}/c^2$ .

## Acknowledgements

The authors thank the SPring-8 staff for their contributions in the operation of the LEPS experiment. This research was supported in part by the Ministry of Education, Science, Sports and Culture of Japan, by the GCOE program in Kyoto University, by the National Science Council of the Republic of China (Taiwan), by the National Research Foundation of Korea (2012R1A2A1A01011926) and by the National Science Foundation (NSF Award PHY-0244999). Author J.D. Parker was supported by a Postdoctoral Fellowship for Foreign Researchers from the Japan Society for the Promotion of Science.

## References

- [1] M. Sato, et al., Phys. Lett. B 659 (2008) 107.
- [2] H. Yim, et al., Phys. Lett. B 688 (2010) 43.
- [3] T. Kishimoto, et al., Nucl. Phys. A 754 (2005) 383.
- [4] T. Kishimoto, et al., Prog. Theor. Phys. Suppl. 168 (2007) 573.
- [5] V.K. Magas, et al., Phys. Rev. C 81 (2010) 024609.
- [6] T. Yamazaki, Y. Akaishi, Phys. Rev. C 76 (2007) 045203.
- [7] Y. Ikeda, T. Sato, Phys. Rev. C 76 (2007) 035203.
- [8] N.V. Shevchenko, A. Gal, J. Mareš, Phys. Rev. Lett. 98 (2007) 082301.
- [9] N.V. Shevchenko, A. Gal, J. Mareš, J. Révai, Phys. Rev. C 76 (2007) 044004.
- [10] Y. Ikeda, H. Kamano, T. Sato, Prog. Theor. Phys. 124 (2010) 533.
- [11] T. Uchino, T. Hyodo, M. Oka, Nucl. Phys. A 868 (2011) 53.
- [12] A. Doté, T. Hyodo, W. Weise, Phys. Rev. C 79 (2009) 014003.
- [13] M. Agnello, et al., Phys. Rev. Lett. 94 (2005) 212303.
- [14] V.K. Magas, et al., Phys. Rev. C 74 (2006) 025206.
- [15] T. Yamazaki, et al., Phys. Rev. Lett. 104 (2010) 132502.
- [16] Y. Oh, C.M. Ko, K. Nakayama, Phys. Rev. C 77 (2008) 045204.
- [17] T. Yamazaki, Y. Akaishi, Phys. Rev. C 76 (2007) 045201.
- [18] N. Muramatsu, arXiv:1201.4094, 2012.
- [19] M. Sumihama, et al., LEPS Collaboration, Phys. Rev. C 73 (2006) 035214.
- [20] M. Lacombe, et al., Phys. Lett. B 101 (1981) 139.
- [21] J. Beringer, et al., Particle Data Group Collaboration, Phys. Rev. D 86 (2012) 010001.
- [22] S.H. Hwanng, et al., LEPS Collaboration, Phys. Rev. Lett. 108 (2012) 092001.